



Biosorption of Ca(II), Cu(II), Pb(II) from aqueous solution by a novel adsorbent of ferric hydroxide-loaded sugar beet pulp

Qiang Liu^a, Ziyuan Gao^a, Na Li^b, Siming Zhu^{a,b,*}

^a School of Food Science and Engineering, South China University of Technology, No. 381 Wushan Road, Guangzhou 510640, China, Tel. +86-20-8711-3668; email: lfsmzhu@scut.edu.cn (S. Zhu), Tel. +86-18718400356; email: 1039107750@qq.com (Q. Liu), Tel. +86-13246838060; email: soovgzy@163.com (Z. Gao)

^b School of Life and Geosciences, Kashgar University, Kashi 844006, China, Tel. +86-18935702769; email: 1690282376/@qq.com (N. Li)

Received 3 April 2019; Accepted 11 September 2019

ABSTRACT

A novel adsorbent was prepared from sugar beet pulp (SBP). SBP was saponified first, then loaded with FeCl₃ and hydrolyzed. The adsorption properties of Ca²⁺, Cu²⁺, and Pb²⁺ by ferric hydroxide-loaded sugar beet pulp (SBPSFH) were studied. The effect of pH, adsorption time, initial concentration of ions, temperature and adsorbent dosage were studied on the adsorption process. In addition, the SBP and SBPSFH were characterized by SEM, XRD and FTIR. The results show that the SBPSFH has significantly improved the uptake of metal ions. At 40°C and pH 4.5–5.0, the adsorption of Ca²⁺, Cu²⁺ and Pb²⁺ by SBPSFH reached the equilibrium within 30 min. The optimal dosage was 10, 10, 5 g L⁻¹, and the maximum adsorption capacity was 21.57, 38.25, 108.18 mg g⁻¹, respectively. The adsorption data fitted well with the pseudo-second-order model and the adsorption isotherm conformed to the Langmuir equation, indicated that the adsorption process is dominated by monomolecular chemical adsorption. The thermodynamic parameters (ΔG° , ΔS° and ΔH°) showed that the adsorption is feasible, spontaneous and endothermic.

Keywords: Adsorption kinetics; Calcium; Copper; Lead; Ferric hydroxide-loaded sugar beet pulp

1. Introduction

Heavy metals have become a major contaminant of water pollution because they exhibit significant biotoxicity at low doses and are easily enriched in the food chain. Metals such as lead, cadmium and copper from mining, metal processing and textile industry have been recognized as hazardous heavy metals. Therefore, the comprehensive treatment of heavy metals wastewater is imminent.

These wastewaters are usually treated with conventional methods such as precipitation [1], ion-exchange technique [2], membrane filtration and electrolysis [3,4]. However, most of the methods have some disadvantages such as sensitive to operational conditions, employment of environmentally

unsafe and expensive chemicals. Compared with the above methods, adsorption is an efficient and simple method for the removal of heavy metals from water. Activated carbon has good adsorption properties, but high cost limits its use in practice. In recent years, a variety of low-cost biomass materials have been used to remove heavy metals and exhibit good adsorption properties.

Beet sugar accounts for about one-third of global sugar. The annual processing of sugar beet produces a large amount of waste pulp. SBP as a feed, no consumption or dry preservation in time will cause waste of resources and environmental pollution. SBP contains about 80% carbohydrates, including pectin, cellulose, hemicellulose and lignin. So SBP

* Corresponding author.

is rich in hydroxyl and carboxyl groups. As a dead cell biosorbent, SBP has good ability of coordinating with metal ions and can be used to treat heavy metals in water, such as Cu^{2+} , Pb^{2+} and Cr^{2+} [5–7].

SBP can also be used as adsorbent after structural modification to enhance its adsorption capacity, such as alkali treatment or saponification of SBP [8,9], high temperature carbonization after phosphoric acid activation [10], mixed treatment of aldehyde and acid [11], direct preparation of activated carbon [12,13], quaternary ammonium modification [14], pectin deacylation [12], etc. It is reported that the SBP structure modified using ferric oxides or other metal oxides has the advantages of larger capacity, faster adsorption and stronger selectivity for removing heavy metal ions than raw SBP [15]. Little attention has been paid to the separation of heavy metal ions by ferric hydroxide modified SBP. In summary, the structural modification of SBP as adsorbent has problems including little attention to the introduction of high price functional groups or the multiple modification of SBP, special modification of a specific adsorbate; few reports are about the physical stability of modified SBP.

The purpose of this study was to modify the SBP through saponification, ferric chloride impregnation and hydrolyzing, to enhance the adsorption capacity of SBP by introducing the ferric hydroxide into SBP. Then the structure of SBPSFH was characterized. The effects of pH value, dosage, temperature and time on the adsorption of Ca^{2+} , Cu^{2+} and Pb^{2+} on SBPSFH were studied. The adsorption equilibrium, kinetics and thermodynamics of isothermal adsorption were studied, and the theoretical adsorption capacity and adsorption mechanism were revealed, which provided a reference and theoretical basis for the utilization of SBPSFH as adsorbent.

2. Materials and methods

2.1. Materials

The chemicals used in this study are listed in Table 1. The sodium hydroxide (NaOH), ferric chloride ($\text{FeCl}_3 \cdot 6\text{H}_2\text{O}$), sodium chloride (NaCl), hydrochloric acid (HCl), copper sulfate ($\text{CuSO}_4 \cdot 5\text{H}_2\text{O}$), lead nitrate (PbNO_3), calcium chloride (CaCl_2), and ethylenediaminetetraacetic acid disodium salt (EDTA-2Na) were of analytical grade and purchased commercially. All the chemicals were used directly without further purifications.

2.2. Modification of SBP

SBP was obtained from the Lvxiang beet sugar Co. Ltd, Xinjiang. SBP was washed using distilled water, filtered and then dried at 55°C for 24 h. SBP was crushed and screened to prepare 150–850 μm size particles. The selected pulp (50 g L^{-1}) was saponified by adding 0.2 mol/L NaOH for 4 h. The saponified SBP (SBPS) was washed using distilled water until the pH of the wastewater did not change again and was dried at 55°C to constant weight. The ferric saponified pulp (SBPSF) was obtained by stirring 50 g/L of saponified pulp in 0.3 mol/L FeCl_3 for 12 h at 30°C . The SBPSF was washed using distilled water until the distilled water was colorless, and then was dried in an oven at 55°C to constant weight. The final product, ferric hydroxide-loaded sugar beet pulp (SBPSFH), was obtained by hydrolysis of 50 g SBPSF in 1 L of 0.2 mol/L NaOH and 12% NaCl for 12 h. After hydrolysis, SBPSFH was washed using distilled water until the effluent acidity did not change again, and dried in an oven at 55°C to constant weight.

2.3. Characterization and analysis

The FT-IR spectra of SBP and SBPSFH were obtained on an FT-IR spectrophotometer (Vector 33-MIR, Germany) to identify the functional groups in the range 4,000–400 cm^{-1} . The X-ray diffraction (XRD) of SBP and SBPSFH was recorded on an automatic X-diffractometer (D/max-III A, Japan) with $\text{Cu K}\alpha$ radiation ($\lambda = 0.154 \text{ nm}$) at room temperature. The morphology of the adsorbent was studied using the scanning electron microscope (EVO 18, Germany).

2.3. Batch adsorption tests

A certain amount of SBPSFH was added into a certain initial concentration of CaCl_2 , $\text{Pb}(\text{NO}_3)_2$ or $\text{CuSO}_4 \cdot 5\text{H}_2\text{O}$ solution. The solution volume of 100 mL was taken for each adsorption test at a given temperature. The pH was not adjusted unless otherwise stated. The bottles were continuously shaken at 125 rpm for 90 min to make sure equilibrium was reached. The effect of the pH was studied by adjusting the pH from 3 to 11 with HCl and NaOH. The influences of adsorbent dose were investigated by adding 0.5 to 3 g of SBPSFH into 100 mL of certain metal ion concentration at 40°C . The kinetic experiments were conducted by mixing a certain adsorbent of given dose and 100 mL of metal ion solution of given concentration

Table 1
Physical properties and purities of chemicals used in this study

Chemical name	CAS number	Formula	Source	Purity (%)
Sodium hydroxide	1310-73-2	NaOH	Tianjin Damao	>96.0 ^a
Ferric chloride	7705-08-0	$\text{FeCl}_3 \cdot 6\text{H}_2\text{O}$	Chemical Industry	99.0 ^a
Sodium chloride	7647-14-5	NaCl	Co. Ltd.	99.5 ^a
Hydrochloric acid	7647-01-0	HCl		36.0 ^a
Copper sulfate	7758-98-7	$\text{CuSO}_4 \cdot 5\text{H}_2\text{O}$		99.0 ^a
Lead nitrate	10099-74-8	PbNO_3		99.0 ^a
Calcium chloride	10043-52-4	CaCl_2		>96.0 ^a
Ethylenediaminetetraacetic acid disodium salt	139-33-3	EDTA-2Na		>99.0 ^a

^aPurities were provided by suppliers. All the chemicals were used directly without further purifications.

for appropriate intervals at 30°C and 40°C. The adsorption isotherm tests were carried out for 90 min at 30°C and 40°C, the initial concentration of the metal ion solutions was adjusted from 200 to 1,400 mg/L, and the usage of adsorbent was 1.0, 1.0, and 0.5 g for Ca^{2+} , Cu^{2+} and Pb^{2+} , respectively. The batch adsorption tests were carried out in duplicates to observe the reproducibility and the average results were used for analysis.

3. Results and discussion

3.1. Characterization of SBP and SBPSFH

3.1.1. SEM analysis

The surface morphology of the SBP and SBPSFH was characterized by SEM (Fig. 1). On the untreated SBP, a smooth surface was observed with many scraps found on the surface. After modification, there were many folds on the surface of SBPSFH and the scraps disappeared completely. These folds increased the surface area of SBP, and were attributed to improve the adsorption capacity of metal ions.

3.1.2. XRD analysis

The XRD patterns of the SBP and SBPSFH are shown in Fig. 2. The weak peaks at 26.48 and 34.76 are the characteristic peaks of ferric hydroxide. The reason for it could be that the impregnated iron is mostly in a coordinated form with various functional groups on SBPSFH, other than in polymeric ferric hydroxide form [16]. The peak value of SBPSFH decreased at $2\theta = 14^\circ\text{--}22^\circ$, indicating that FeCl_3 and NaOH solutions make the crystal structure changed. At $2\theta = 16^\circ$, the low-crystallinity polysaccharide structure has a weak peak, while at 22° it has a highly crystalline cellulose peak. The decrease in the peak value after the modification indicates that the modification causes the crystal structure of the beet pulp to be destroyed, leaving more reactive groups exposed, facilitating the combination with metal ions and improving the adsorption performance of SBP.

3.1.3. FTIR spectral analysis

From the FTIR spectra (Fig. 3) of SBP and SBPSFH, some changes have taken place between them. The band

at 894.46 cm^{-1} was assigned to the Fe-OH bending vibration. This band is the characteristic peaks of ferric hydroxide of SBPSFH. A band at $1,047.45\text{ cm}^{-1}$ corresponds to C-O

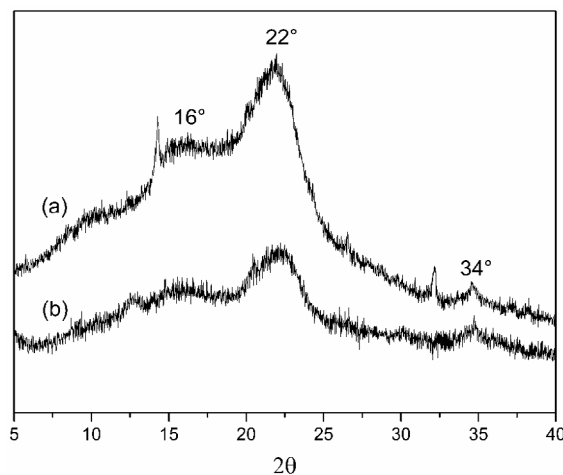


Fig. 2. XRD of SBP (a) and SBPSFH (b).

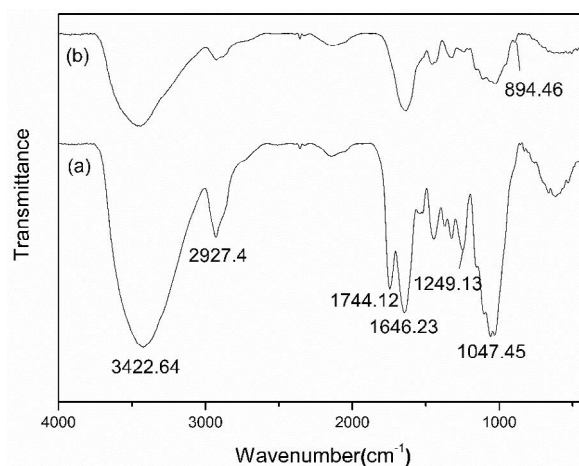


Fig. 3. FTIR of SBP (a) and SBPSFH (b).

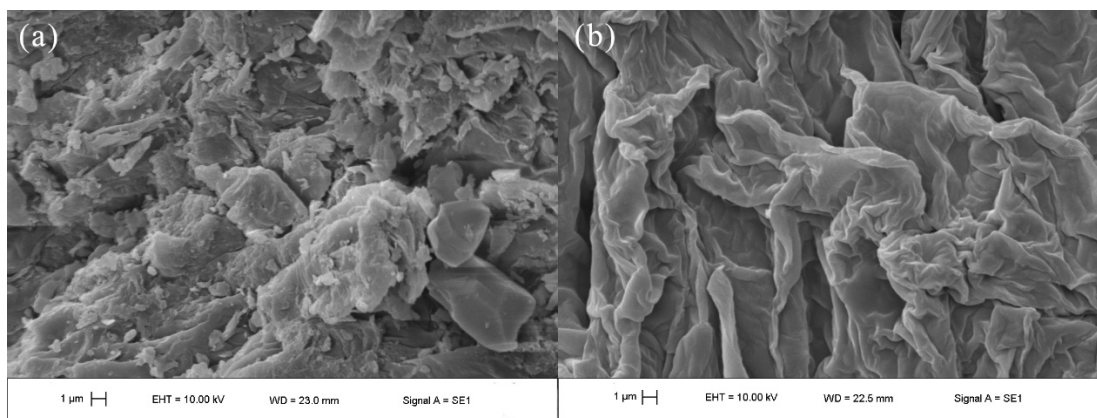


Fig. 1. SEM of SBP (a) and SBPSFH (b).

bond in hemicellulose and cellulose [17]. The weak band at $1,249.13\text{ cm}^{-1}$ indicates the presence of C=O bond of a carboxylate group. The bands detected at $1,646.23$ and $1,744.12\text{ cm}^{-1}$ correspond to the C=O bond of the carboxylic group [18]. The peak at $1,744.12\text{ cm}^{-1}$ was disappeared in the FTIR spectrum of SBPSFH, indicating that ester bonds were destroyed during the modification. The absorption at $3,422.64\text{ cm}^{-1}$ is due to the O–H stretching and that at $2,927.94\text{ cm}^{-1}$ is due to the C–H stretching [19]. Thus, the effect of the modification is to destroy the glycosidic bonds in the sugar beet pulp cellulose, to obtain more hydroxyl groups, and to load the iron onto more hydroxyl and carboxylate groups. The adsorption of metal ions by SBP has been greatly improved after the modification.

3.2. Effect of solution pH

Fig. 4 shows the metal ions adsorption capacity of the SBPSFH as a function of pH. In a certain pH range, the adsorption capacity of three ions increases as the pH increases. The effect of pH on the adsorption of Pb^{2+} is significantly greater than that of Cu^{2+} and Ca^{2+} . The metal cations removal increased significantly from pH 3.0 to 5.0. The surface of the adsorbent carries a large amount of negative charges from the carboxyl and hydroxyl groups. At low pH, the surface of SBPSFH would be surrounded by hydronium ions. The existing H^+ reduces the metal ion interaction with binding sites of the adsorbent by greater repulsive forces [20]. The solution contains a large amount of H^+ , because of its smaller diameter, it is easier to combine with the oxygen-containing functional group adsorption site of the adsorbent, and has a strong competitive relationship with metal ions, weakening the adsorption capacity of metal ions. In addition, according to the theory of chemical reaction, H^+ has more superiority to combine with the adsorption site under low pH. The pH value not only affects the charge on the surface of SBPSFH but also influences the degree of ionization and the presence of ions in the solution. The dominant species of lead in the pH range 3–5 are Pb^{2+} and PbOH^+ , while the lead above pH 6.0 occurs as insoluble $\text{Pb}(\text{OH})_2$. Within the range of pH 3–5, as the pH value increases, the negative charge on the surface of the adsorbent and the dissociation degree

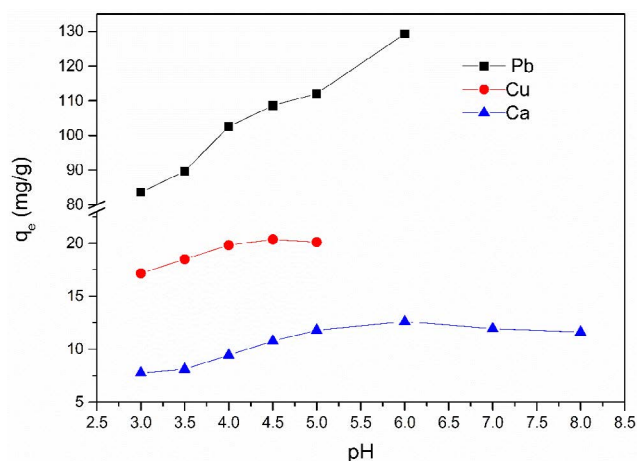


Fig. 4. Effect of initial pH on adsorption of Ca^{2+} , Cu^{2+} , Pb^{2+} .

of the oxygen-containing functional group such as $-\text{COOH}$ increase, and further deprotonation benefits to further combine with the metal ions onto SBPSFH. Thus, the adsorption increases under high solution pH. The similar phenomenon occurs for the solution of Cu^{2+} or Ca^{2+} . The dramatic decrease in Pb^{2+} adsorption above pH 6.0 was probably due to the precipitation of Pb^{2+} as insoluble $\text{Pb}(\text{OH})_2$.

3.3. Effect of adsorbent dose

Effect of adsorbent dose on the removal of Ca^{2+} , Cu^{2+} and Pb^{2+} is shown in Fig. 5. With the increase of adsorption dose, the removal of metal ions has a significant increase, but the equilibrium adsorption capacity (q_e) has been decreasing. The reason for it is that increasing the amount of adsorbent can effectively increase the total number of functional groups and adsorption sites benefit to the adsorption reaction, so the adsorption of metal ions increases. As for the trend of a decrease in equilibrium adsorption capacity, it may be due to electrostatic repulsion effect between the binding sites of the adsorbent. The system reaches the adsorption equilibrium at lower values of relative adsorption indicating the adsorption sites remain unsaturated [21].

3.4. Effect of the contact time and the initial concentration of metal ions

Fig. 6 depicts the effect of contact time (a) and the initial concentration (b) on metal ions adsorption onto SBPSFH. The adsorption process can be roughly divided into three stages, rapid, slow and equilibrium. In the fast adsorption phase, the adsorption of Ca^{2+} , Cu^{2+} and Pb^{2+} by the adsorbent was 96.94%, 96.50% and 87.65% of the saturated adsorption capacity within 5 min, respectively. The adsorption of metal ions onto SBPSFH reached equilibrium within 30 min. At the beginning of adsorption, there are many adsorption sites existing on the surface of the adsorbent, and the competition of the metal ions on the adsorption sites is weak, and the initial concentration gradient of the ions is larger, resulting in greater driving force for adsorption and accelerating the adsorption rate. As the adsorption sites on the adsorbent surface are gradually occupied, the

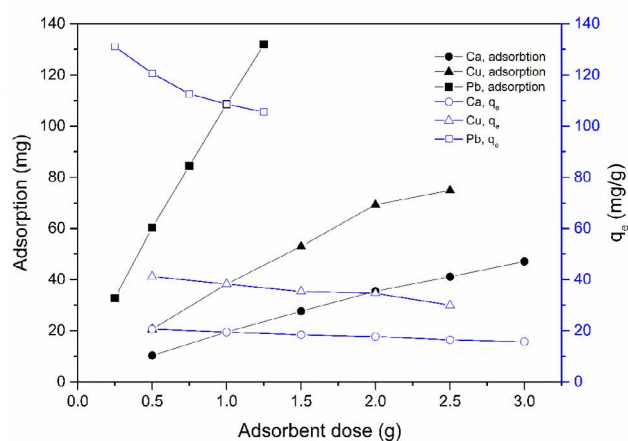


Fig. 5. Effect of adsorbent dose on adsorption of Ca^{2+} , Cu^{2+} , Pb^{2+} .

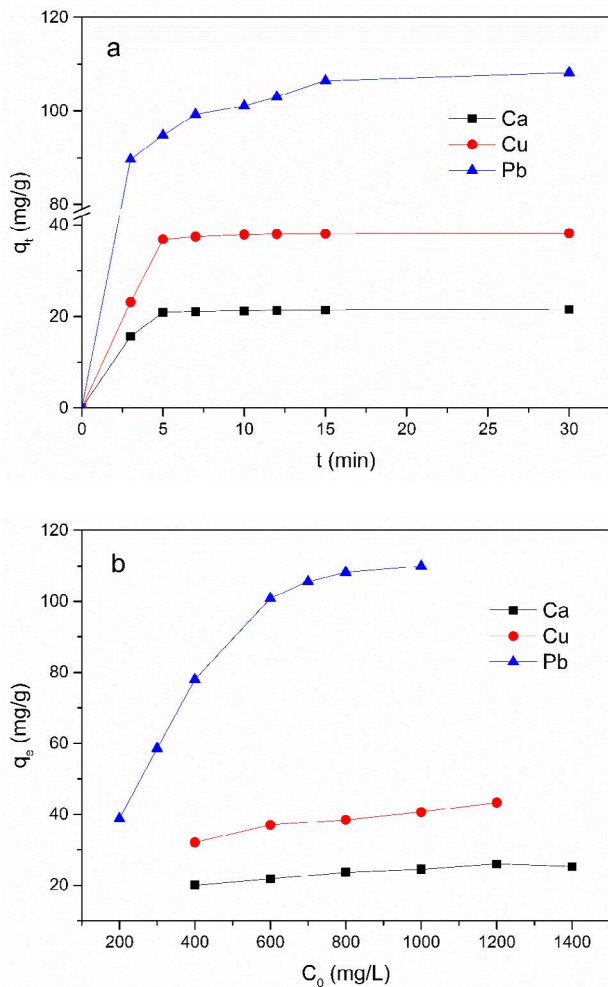


Fig. 6. Effect of time (a) and initial concentration and (b) on the adsorption of Ca²⁺, Cu²⁺, Pb²⁺.

adsorption rate depends on the rate at which the metal ions enter the inside of the micropores [12] and the adsorption rate is slowed due to the increased resistance. The equilibrium adsorption did not change with further increase in initial metal ion concentration showing a saturation trend at higher metal ions concentrations due to a finite number of surface binding sites [20].

3.5. Adsorption kinetics

Two adsorption kinetic models were used to describe the adsorption kinetics and rate limiting step in this paper [22–24].

At first, q_t is given by Eq. (1):

$$q_t = (C_0 - C_t) \cdot \frac{V}{m} \quad (1)$$

The pseudo-first order model is given by Eqs. (2) and (3):

$$\frac{dq}{dt} = k_1(q_e - q_t) \quad (2)$$

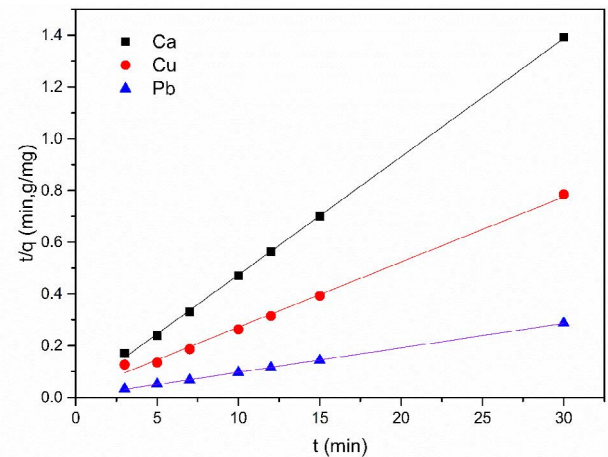


Fig. 7. Pseudo-second order reaction equation of SBPSFH adsorbing Ca²⁺, Cu²⁺, Pb²⁺ (313.15 K).

$$\ln(q_e - q_t) = \ln q_e - \frac{k_1}{2.303} t \quad (3)$$

The pseudo-second order model can be expressed by Eqs. (4) and (5):

$$\frac{dq}{dt} = k_2(q_e - q_t)^2 \quad (4)$$

$$\frac{t}{q_t} = \frac{1}{k_2 q_e^2} + \frac{t}{q_e} \quad (5)$$

where C_0 and C_t are the metal ion concentration (mg L⁻¹) in initial and at time t , respectively; m is the weight of adsorbent (g); V is the volume of the solution (l); q_e and q_t are the amount of metal adsorbed per unit weight of adsorbent (mg g⁻¹) at equilibrium, and at time t , respectively; and k_1 and k_2 are the adsorption rate constants of two models.

The results obtained for adsorption process of Ca²⁺, Cu²⁺ and Pb²⁺ onto SBPSFH was fitted to Eqs. (3) and (5). The fitting results are shown in Fig. 7 and the model fitting parameters are shown in Table 2. The better model representing sorption of metal ions onto SBPSFH was based on a pseudo-second order process, and R^2 was as high as 99.96%, 99.77% and 99.98% for Ca²⁺, Cu²⁺ and Pb²⁺, respectively. The theoretical adsorption capacity determined by the pseudo-second order kinetic model is closer to the experimental data than by the pseudo-first order kinetics model, indicating that the adsorption of metal ions in SBPSFH is mainly chemisorption mechanism [25].

3.6. Adsorption isotherms

Two equilibrium models were used to describe adsorption isotherm relationships in this paper [26–28]. The sorption equilibrium data for the single metal system were fitted to the Langmuir (Eq. (6)) and Freundlich models (Eq. (7)):

$$\frac{C_e}{q_e} = \frac{1}{K_L q_m} + \frac{C_e}{q_m} \quad (6)$$

Table 2
Adsorption kinetic parameters

Ion	C_0 /(mg L ⁻¹)	T /(K)	Pseudo-first order model			Pseudo-second order model		
			q_e /(mg g ⁻¹)	k_1 /min ⁻¹	R^2	q_e /(mg g ⁻¹)	k_2 /(mg g ⁻¹ min ⁻¹)	R^2
Ca ²⁺	600	303.15	8.85	0.6880	0.8837	20.05	0.0762	0.9991
		313.15	3.52	0.5140	0.7637	21.91	0.1185	0.9996
Cu ²⁺	800	303.15	18.63	0.4734	0.9167	39.32	0.0180	0.9977
		313.15	16.29	0.8569	0.8419	39.71	0.0315	0.9945
Pb ²⁺	800	303.15	52.28	0.9120	0.9555	106.16	0.0238	0.9997
		313.15	34.09	0.4131	0.9202	111.23	0.0107	0.9998

$$\ln q_e = \frac{1}{n} \ln C_e + \ln K_f \quad (7)$$

$$R_L = \frac{1}{1 + K_L C_0} \quad (8)$$

where q_m (mg g⁻¹) is the maximum adsorption capacity per unit mass of adsorbent corresponding to complete monolayer coverage; q_e (mg g⁻¹) is the maximum amount of adsorbate adsorbed per unit mass of adsorbent at equilibrium; R_L is the separation factor, indicating whether the type of the isotherm is favorable ($0 < R_L < 1$), unfavorable ($R_L > 1$), linear ($R_L = 1$), or irreversible ($R_L = 0$); C_0 (mg L⁻¹) is the initial metal ion concentration, C_e (mg L⁻¹) is the concentration of adsorbate at equilibrium; K_L is the constant of the Langmuir isotherm; K_f and n are the constants related to the adsorption capacity and the adsorption intensity of Freundlich isotherm, respectively.

The Langmuir and Freundlich models were used to depict the adsorption equilibrium of metal ions on SBPSFH to do this, operating temperature and module constants calculated by the isotherms were used to get the adsorptive capacity of SBPSFH. Fig. 8 shows the adsorption isotherms for Ca²⁺, Cu²⁺ and Pb²⁺ (q_e vs. C_e). The experimental data were fitted to Eqs. (6) and (8), the isotherm constants are given in Table 3. Comparing the results (Table 3) of Langmuir and Freundlich model fitted, the Langmuir model is better than the Freundlich model, because R^2 value of the Langmuir model is greater than that of the Freundlich model. The difference between the actual adsorption capacity and the theoretical adsorption capacity calculated by the Langmuir model is not significant, indicating that the adsorption mechanism is based on monolayer adsorption. As for the curve of Ca²⁺ and Cu²⁺, the R^2 value fitted by the Freundlich model is greater than 0.9563, indicating that there is a certain non-uniform multi-layer adsorption. Furthermore, Table 2 shows the R_L values of the Langmuir model are between 0 and 1, and the Freundlich constants of $1/n$ are smaller than 1, indicating the adsorption of Ca²⁺, Cu²⁺ and Pb²⁺ by SBPSFH is a favorable nature of biosorption [29]. Pb²⁺ shows higher sorption capacity and binding ability on SBPSFH compared with Ca²⁺ and Cu²⁺.

3.7. Thermodynamic study

The thermodynamic parameters such as the Gibbs free energy ΔG° , enthalpy ΔH° and entropy changes ΔS° for the adsorption process were calculated by the following equations [17,30,31],

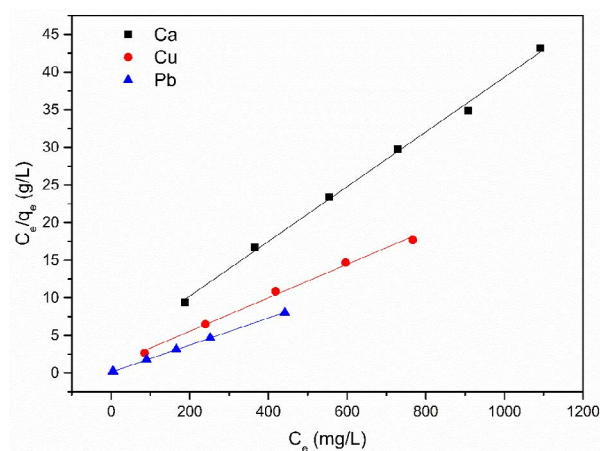


Fig. 8. Langmuir adsorption isothermal curve fit of modified SBP adsorbing Ca²⁺, Cu²⁺, Pb²⁺ (313.15 K).

$$\Delta G^\circ = -RT \ln Kc \quad (9)$$

$$Kc = q_e / C_e \quad (10)$$

$$\Delta G^\circ = \Delta H^\circ - T \Delta S^\circ \quad (11)$$

$$\ln Kc = \Delta S^\circ / R - \Delta H^\circ / RT \quad (12)$$

where the R is universal gas constant (8.314 J mol⁻¹ K⁻¹); Kc is equilibrium constant, and T is absolute temperature (K). Table 4 shows the thermodynamic parameters for metals adsorption by SBPSFH. The enthalpy changes for Ca²⁺, Cu²⁺, Pb²⁺ adsorption by SBPSFH calculated by the slope of $\ln Kc$ vs. $1/T$ was found to be 0.23, 0.06, 0.49 kJ mol⁻¹, respectively. The positive value of ΔH° suggests the endothermic adsorption nature, which is supported by the increasing metal ions uptake with the increase of temperature [17]. The negative sign of ΔG° indicates the spontaneous nature of metal ions uptake onto SBPSFH [10,32]. Entropy changes (ΔS°) of the adsorption reaction of Ca²⁺, Cu²⁺, Pb²⁺ adsorption were calculated to be 0.91, 0.28, 1.90 J mol⁻¹ K⁻¹. The positive ΔS° value suggests an increase in the randomness at solid/solution interface during the adsorption process [13].

3.8. Adsorption mechanisms

SBPSFH was prepared by the saponification of SBP, then iron-load reaction and then the Fe³⁺ hydrolysis of the

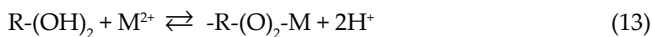
Table 3
Fitting parameters of isothermal adsorption model

ion	T/(K)	Langmuir			Freundlich			
		$q_m/(\text{mg g}^{-1})$	$K_L/(\text{L mg}^{-1})$	R^2	R_L	$K_f/(\text{mg}^{1-n} \text{g}^{-1} \text{L}^{-n})$	$1/n$	R^2
Ca ²⁺	303.15	25.54	0.010	0.9980	0.0667–0.2000	7.59	0.1619	0.9787
	313.15	27.48	0.012	0.9968	0.0562–0.1724	9.26	0.1474	0.9563
Cu ²⁺	303.15	43.27	0.021	0.9955	0.0382–0.1064	19.09	0.1142	0.9687
	313.15	44.95	0.020	0.9942	0.0400–0.1111	18.23	0.1273	0.9705
Pb ²⁺	303.15	106.84	0.217	0.9986	0.0046–0.0225	46.00	0.1502	0.7081
	313.15	110.99	0.161	0.9972	0.0062–0.0301	43.02	0.1695	0.7647

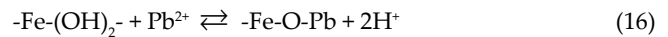
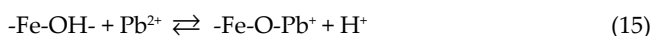
Table 4
Thermodynamic parameters for metal ions uptake by SBPSFH

Ion	T/K	$\Delta G^\circ/(\text{kJ mol}^{-1})$	$\Delta H^\circ/(\text{kJ mol}^{-1})$	$\Delta S^\circ/(\text{J mol}^{-1} \text{K}^{-1})$
Ca ²⁺	293.15	-2.58	0.23	0.91
	303.15	-3.43		
	313.15	-3.82		
Cu ²⁺	293.15	-1.38	0.06	0.28
	303.15	-1.60		
	313.15	-1.76		
Pb ²⁺	293.15	-4.82	0.49	1.90
	303.15	-6.19		
	313.15	-7.44		

iron-loaded SBP. After the aforesaid process, the crystal structure of SBP changed, leaving more functional groups exposed, such as hydroxyl, carbonyl, etc. These groups are easily combined with metal ions and the raised ions uptake indicates the success of modification. As the pH increases from 3 to 5, the adsorption capacity increases (Fig. 3). The reason for it is due to the synergistic effect of several different adsorption mechanisms present at the ion uptake process. One is ion exchange between functional groups such as hydroxyl, carboxyl and metal ions on the surface of SBPSFH. The possible reaction process is as follows [33]:



At low pH, the relatively high concentration of H⁺ inhibits the ionization of the hydroxyl and carboxyl groups of the SBPSFH, thereby weakening the exchange capacity of the hydroxyl and carboxyl groups for heavy metals. As the pH increases, the ionization degree of the two groups and the electronegativity gradually increases, so the exchange capacity of SBPSFH are also enhanced. In addition, the ferric hydroxide-loaded SBP also have good coordination properties. The hydroxyl groups bind to the iron of SBPSFH can also form a monodentate or double-dentate complex with heavy metal ions in solution. The possible reaction process is as follows [7,34]:



With the synergistic effect of these groups, the adsorption performance of modified beet pulp was greatly improved.

4. Conclusions

In this study, the adsorption capacity of SBP has been significantly improved after ferric hydroxide loaded modification. The theoretical maximum absorptions of Ca²⁺, Cu²⁺ and Pb²⁺ were 27.48, 44.95 and 110.99 mg g⁻¹, respectively, while the raw beet pulp had only 4.70, 10.16 and 32.89 mg g⁻¹, respectively. SBPSFH has been used successfully as a good adsorbent for removal of metal ions from wastewater in our work. Adsorption process was affected by various parameters such as solution pH, contact mode and contact time. The adsorption of Ca²⁺, Cu²⁺ and Pb²⁺ increased with the increase of solution pH, and the adsorption amount was the largest at 4.5–5. With the increase of adsorbent dose, the removal of metal ions increased significantly, but the equilibrium adsorption capacity decreased.

The adsorption of Ca²⁺, Cu²⁺ and Pb²⁺ by SBPSFH could be depicted better by the Langmuir isotherm model within the experimental concentration range. So the possible adsorption mechanism of SBPSFH is mainly based on monolayer adsorption. The thermodynamic parameters (ΔG° , ΔS° and ΔH°) showed that the adsorption was feasible, spontaneous and endothermic.

The adsorption rate of Ca²⁺, Cu²⁺ and Pb²⁺ by SBPSFH is very rapid during the initial period of time. At the first 15 min, the adsorption saturation degree has reached more than 98%, and adsorption equilibrium is reached after 30 min. Compared with the pseudo-first order kinetics model, the pseudo-second order kinetics model can better fit the dynamic adsorption process of metal ions by SBPSFH, and the correlation coefficient is above 99.54%. This indicates that the adsorption of metal ions in SBPSFH is mainly ascribed to chemisorption mechanism.

In conclusion, under the synergistic effect of diverse functional groups, the adsorption performance of modified beet pulp of SBPSFH has been greatly improved. The high performance indicated that SBPSFH is a promising material for metal ions removal.

Funding sources

This work was financially supported by the National Natural Science Foundation of China (NSFC) foundation (U1203183), the Natural Science Foundation of Xinjiang

Province, China (2018D01A03), the Science and Technology Innovation team's construction Foundation in Xinjiang Uygur Autonomous Region (2014751002) and the Science and Technology Planning Project of Guangdong Province, China (2014A020209019 and 2015A020210039).

Acknowledgments

The authors are grateful for the technical support from the Analytical and Testing Center, South China University of Technology, Guangzhou, China.

References

- [1] K. Zhou, L. Pan, C. Peng, D. He, C. Wei, Selective precipitation of Cu in manganese-copper chloride leaching liquor, *Hydrometallurgy*, 175 (2018) 319–325.
- [2] M. Naushad, A. Mittal, M. Rathore, V. Gupta, Ion-exchange kinetic studies for Cd(II), Co(II), Cu(II), and Pb(II) metal ions over a composite cation exchanger, *Desal. Wat. Treat.*, 54 (2015) 2883–2890.
- [3] A. Almasian, M. Giyahi, G.C. Fard, S.A. Dehdast, L. Maleknia, Removal of heavy metal ions by modified PAN/PANI-nylon core-shell nanofibers membrane: filtration performance, antifouling and regeneration behavior, *Chem. Eng. J.*, 351 (2018) 1166–1178.
- [4] S. Mulyati, N. Arahman, Syawaliah, Mukramah, Removal of metal iron from groundwater using aceh natural zeolite and membrane filtration, *IOP Conference Series Materials Science and Engineering*, Vol. 180, 2017, p. 012128.
- [5] E. Pehlivan, B.H. Yanik, G. Ahmetli, M. Pehlivan, Equilibrium isotherm studies for the uptake of cadmium and lead ions onto sugar beet pulp, *Bioresour. Technol.*, 99 (2008) 3520–3527.
- [6] E. Pehlivan, S. Cetin, B.H. Yanik, Equilibrium studies for the sorption of zinc and copper from aqueous solutions using sugar beet pulp and fly ash, *J. Hazard. Mater.*, 135 (2006) 193–199.
- [7] M.T. Samadi, A.R. Rahman, M. Zarrabi, E. Shahabi, F. Sameei, Adsorption of chromium (VI) from aqueous solution by sugar beet bagasse-based activated charcoal, *Environ. Technol.*, 30 (2009) 1023–1029.
- [8] J. Zolgharnein, N. Asanjarani, T. Shariatmanesh, Removal of thallium(I) from aqueous solution using modified sugar beet pulp, *Toxicol. Environ. Chem.*, 93 (2011) 207–214.
- [9] H. Arslanoglu, F. Tumen, A study on cations and color removal from thin sugar juice by modified sugar beet pulp, *J. Food Sci. Technol.*, 49 (2012) 319–327.
- [10] A. Ozer, F. Tumen, Cd(II) adsorption from aqueous solution by activated carbon from sugar beet pulp impregnated with phosphoric acid, *Fresen. Environ. Bull.*, 12 (2003) 1050–1058.
- [11] H.S. Altundogan, N. Bahar, B. Mujde, F. Tumen, The use of sulphuric acid-carbonization products of sugar beet pulp in Cr(VI) removal, *J. Hazard. Mater.*, 144 (2007) 255–264.
- [12] D. Li, J. Yan, Z. Liu, Z. Liu, Adsorption kinetic studies for removal of methylene blue using activated carbon prepared from sugar beet pulp, *Int. J. Environ. Sci. Technol.*, 13 (2016) 1815–1822.
- [13] G. Dursun, H. Çiçek, A.Y. Dursun, Adsorption of phenol from aqueous solution by using carbonised beet pulp, *J. Hazard. Mater.*, 125 (2005) 175–182.
- [14] S. Tunali Akar, S. Celik, D. Tunc, Y. Yetimoglu Balk, T. Akar, Biosorption potential of surface-modified waste sugar beet pulp for the removal of Reactive Yellow 2 (RY2) anionic dye, *Turk. J. Chem.*, 40 (2016) 1044–1054.
- [15] J.A. Munoz, A. Gonzalo, M. Valiente, Arsenic adsorption by Fe(III)-loaded open-celled cellulose sponge. Thermodynamic and selectivity aspects, *Environ. Sci. Technol.*, 36 (2002) 3405–3411.
- [16] Z.M. Gu, J. Fang, B.L. Deng, Preparation and evaluation of GAC-based iron-containing adsorbents for arsenic removal, *Environ. Sci. Technol.*, 39 (2005) 3833–3843.
- [17] M. Moyo, U. Guyo, G. Mawenyiyo, N.P. Zinyama, B.C. Nyamunda, Marula seed husk (*Sclerocarya birrea*) biomass as a low cost biosorbent for removal of Pb(II) and Cu(II) from aqueous solution, *J. Ind. Eng. Chem.*, 27 (2015) 126–132.
- [18] W. Lan, C.-F. Liu, R.-C. Sun, Fractionation of bagasse into cellulose, hemicelluloses, and lignin with ionic liquid treatment followed by alkaline extraction, *J. Agric. Food Chem.*, 59 (2011) 8691–8701.
- [19] C.H. Wu, C.Y. Kuo, S.S. Guan, Adsorption of heavy metals from aqueous solutions by waste coffee residues: kinetics, equilibrium, and thermodynamics, *Desal. Wat. Treat.*, 57 (2016) 5056–5064.
- [20] Z. Aksu, I.A. Isoglu, Removal of copper(II) ions from aqueous solution by biosorption onto agricultural waste sugar beet pulp, *Process Biochem.*, 40 (2005) 3031–3044.
- [21] B.M.W.P.K. Amarasinghe, R.A. Williams, Tea waste as a low cost adsorbent for the removal of Cu and Pb from wastewater, *Chem. Eng. J.*, 132 (2007) 299–309.
- [22] L. Jiang, H. Yu, X. Zhou, X. Hou, Z. Zou, S. Li, C. Li, X. Yao, Preparation, characterization, and adsorption properties of magnetic multi-walled carbon nanotubes for simultaneous removal of lead(II) and zinc(II) from aqueous solutions, *Desal. Wat. Treat.*, 57 (2015) 18446–18462.
- [23] Y.-S. Ho, A.E. Ofomaja, Kinetic studies of copper ion adsorption on palm kernel fibre, *J. Hazard. Mater.*, 137 (2006) 1796–1802.
- [24] Q. Huang, S.-m. Zhu, D. Zeng, S.-j. Yu, Kinetic and thermodynamic study of the adsorption of calcium onto sugar beet pulp, *Sugar Ind.*, 141 (2016) 565–570.
- [25] V.M. Vučurović, R.N. Razmovski, M.N. Tekić, Methylene blue (cationic dye) adsorption onto sugar beet pulp: equilibrium isotherm and kinetic studies, *J. Taiwan Inst. Chem. Eng.*, 43 (2012) 108–111.
- [26] S. Raghav, D. Kumar, Adsorption equilibrium, kinetics, and thermodynamic studies of fluoride adsorbed by tetrametallic oxide adsorbent, *J. Chem. Eng. Data*, 63 (2018) doi: acs.jced.8b00024.
- [27] Z.Y. Gao, Y.T. Wang, B.B. Xu, S.M. Zhu, Adsorption mechanism of alkali-earth metal ions from aqueous solutions by using hydrated ferric oxide-loaded Chinese Kulumuti tea residue, *Fresen. Environ. Bull.*, 27 (2018) 4802–4812.
- [28] M.R. Malekbala, S. Hosseini, S.K. Yazdi, S.M. Soltani, M.R. Malekbala, The study of the potential capability of sugar beet pulp on the removal efficiency of two cationic dyes, *Chem. Eng. Res. Des.*, 90 (2012) 704–712.
- [29] L. Wang, J. Zhang, R. Zhao, Y. Li, C. Li, C. Zhang, Adsorption of Pb(II) on activated carbon prepared from *Polygonum orientale* Linn.: kinetics, isotherms, pH, and ionic strength studies, *Bioresour. Technol.*, 101 (2010) 5808–5814.
- [30] K. Saltali, A. Sari, M. Aydin, Removal of ammonium ion from aqueous solution by natural Turkish (Yildizeli) zeolite for environmental quality, *J. Hazard. Mater.*, 141 (2007) 258–263.
- [31] D. Han, Z. Zhao, Z. Xu, Y. Li, P. Zhang, X. Guo, beta-FeOOH-coupled activated carbon prepared by the high temperature impregnation method for bromate removal from water, *J. Chem. Eng. Data*, 63 (2018) 2243–2251.
- [32] A. Sari, M. Tuze, O.D. Ulucelue, M. Soylak, Biosorption of Pb(II) and Ni(II) from aqueous solution by lichen (*Cladonia furcata*) biomass, *Biochem. Eng. J.*, 37 (2007) 151–158.
- [33] V.M. Dronnet, C.M.G.C. Renard, M.A.V. Axelos, J.F. Thibault, Binding of divalent metal cations by sugar-beet pulp, *Carbohydr. Polym.*, 34 (1997) 73–82.
- [34] S. Schalow, H. Gohm, D. Chico, S. Soyka, Biological Ion-Exchangers from Sugar Beet Pulp, *Scientific Works of the University of Food Technologies - Plovdiv*, 2009.